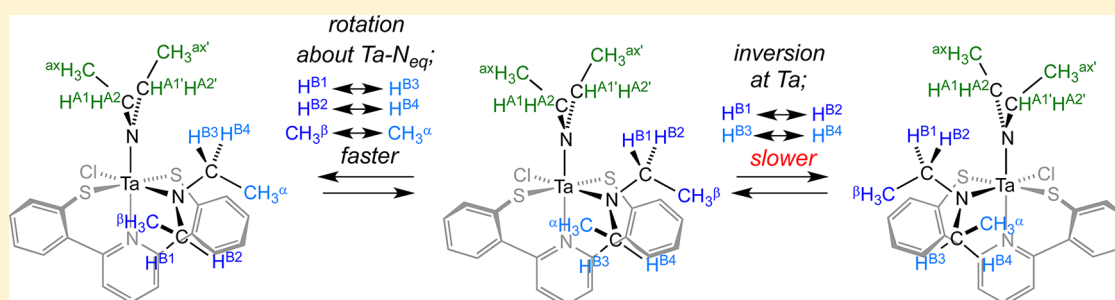


# Synthesis of a Bis(thiophenolate)pyridine Ligand and Its Titanium, Zirconium, and Tantalum Complexes

Taylor N. Lenton, David G. VanderVelde, and John E. Bercaw\*

Arnold and Mabel Beckman Laboratories of Chemical Synthesis, California Institute of Technology, Pasadena, California 91125, United States

## Supporting Information



**ABSTRACT:** A precursor to a new tridentate  $LX_2$  type ligand, bis(thiophenol)pyridine ((SNS) $H_2$  = (2- $C_6H_4SH$ ) $_2$ -2,6- $C_5H_3N$ ), was prepared. Bis(thiophenolate)pyridine complexes of Ti, Zr, and Ta having dialkylamido coligands were synthesized and structurally characterized. The zirconium complex (SNS)Zr(NMe $_2$ ) $_2$  (**4**) displays  $C_2$  symmetry in the solid state, unlike a related bis(phenolate)pyridine compound,  $C_s$ -symmetric (ONO)Ti(NMe $_2$ ) $_2$ . This change is likely the result of strain about the sulfur atom in the six-membered chelate with longer metal–sulfur and carbon–sulfur bonds. Solid-state structures of tantalum complexes (SNS)Ta(NMe $_2$ ) $_3$  (**5**) and (SNS)TaCl(NEt $_2$ ) $_2$  (**6**) also display pronounced  $C_2$  twisting of the SNS ligand. 1D and 2D NMR experiments show that **5** is fluxional, with rotation about the Ta–N(amido) bonds occurring on the NMR time scale that interchange the equatorial amide methyl groups ( $\Delta G^\ddagger_{393} = 25.0(3)$  kcal/mol). The fluxional behavior of **6** in solution was also studied by variable-temperature  $^1H$  NMR. Observation of separate signals for the diastereotopic protons of the methylene unit of the diethylamide indicates that the complex remains locked on the NMR time scale in one diastereomeric conformation at temperatures below  $-50$  °C, fast rotation about the equatorial amide Ta–N bonds occurs at higher temperature ( $\Delta G^\ddagger_{393} = 13.4(3)$  kcal/mol), and exchange of diastereomeric methylene protons occurs via inversion at Ta that interconverts antipodes ( $\Delta G^\ddagger_{393} \approx 14(1)$  kcal/mol).

## INTRODUCTION

A substantial amount of the organometallic chemistry of early d-block transition metals has been developed using a metallocene platform. Metallocenes have relatively well-defined frontier orbitals and coordination sites restricted to the equatorial plane. With this predictable geometric arrangement for metallocene complexes, the mechanisms of many fundamental transformations have been elucidated. For the same reasons, polyolefin catalysts based on metallocenes have been extensively investigated.<sup>1</sup> Predictable changes in molecular weight, polymer stereochemistry, and comonomer incorporation have been achieved by variations in the structures of variously substituted metallocenes, particularly *ansa*-metallocenes of group 4 metals.<sup>2</sup> More recently non-metallocene (or “post-metallocene”) single-site catalysts have been developed. These offer advantages as compared to metallocene catalysts, such as relative ease of ligand synthesis, more general metalation of the ligand, and the potential to effect new types of stereocontrolled polymerizations.<sup>3</sup> We have previously described precatalysts having a pincer ligand framework of the  $LX_2$  type, bis(phenolate)pyridine (ONO = pyridine-2,6-bis-

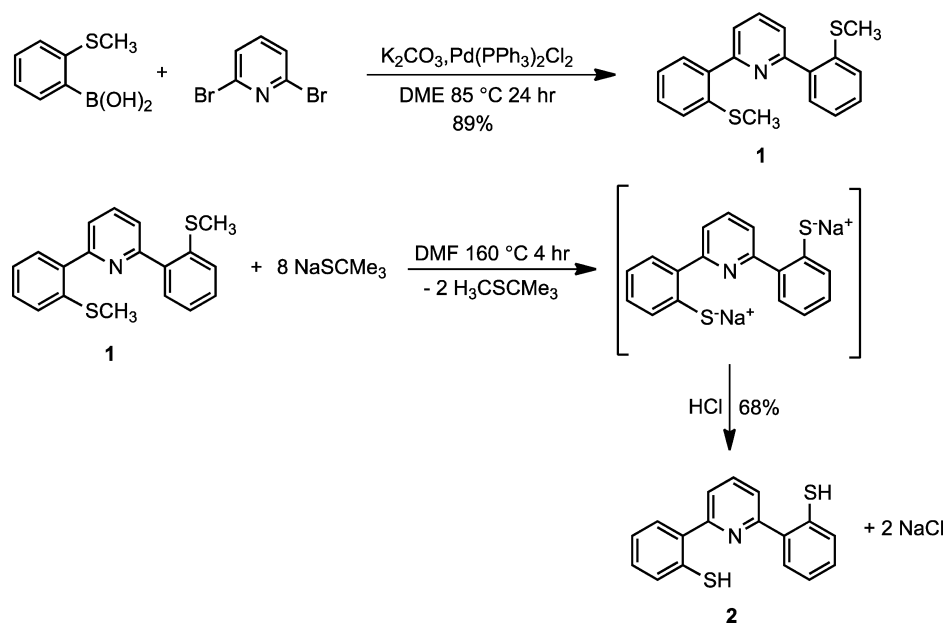
(4,6- $t$ Bu $_2$  phenolate). ONO ligands normally coordinate in a meridional fashion, and depending upon the relative twisting of phenolate rings, (ONO)MX $_2$  complexes may adopt  $C_1$ ,  $C_s$ ,  $C_2$ , or  $C_{2v}$  symmetry with frontier orbitals similar to those of metallocenes.<sup>3a,4</sup> Early experiments revealed that group 4 ONO complexes exhibit moderate to good activities for ethylene and propylene polymerization.<sup>4,5</sup> Stereoirregular polypropylene is commonly produced due to racemization of the catalyst site, likely a consequence of similar energies of the  $C_2$ ,  $C_{2v}$ , and  $C_s$  isomers and their facile interconversions. We reasoned that, with a more rigid ligand system, stereoregular polyolefins might be obtained.<sup>6,7</sup>

A modified pincer ligand, bis(thiophenolate)pyridine (SNS), was anticipated to offer a possible solution, because the larger sulfur atom would increase ring strain in the metal chelate and lead to a stronger preference for a twisted  $C_2$  as opposed to a flat  $C_{2v}$  geometry. Indeed, the analogous early-transition-metal complexes with a bis(phosphido)pyridine (PNP) ligand display

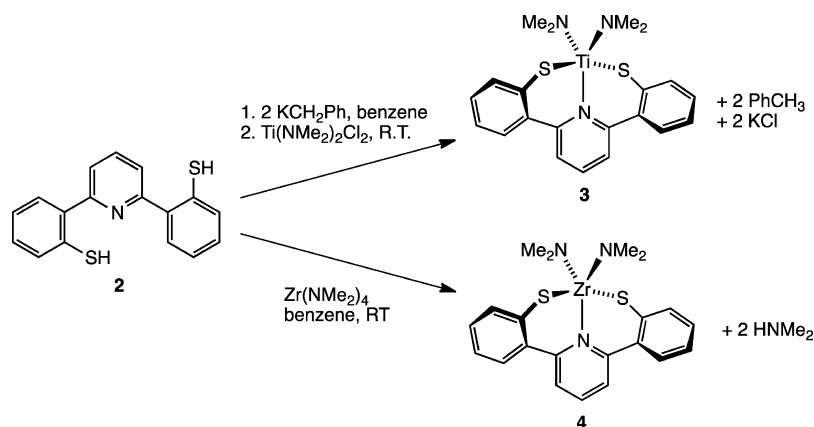
Received: August 15, 2012

Published: October 18, 2012

Scheme 1



Scheme 2



very twisted  $C_2$  symmetry, as compared with the bis(anilide)-pyridine (NNN) complexes, due to the long metal-phosphorus and carbon-phosphorus (*vis-à-vis* M–N and C–N) bonds.<sup>13b</sup> Examples of group 4 and 5 transition metals bearing anionic thiolate ligands are relatively rare, and their scarcity has been attributed to a hard/soft mismatch.<sup>8</sup> Most examples of early-transition-metal thiolates have cyclopentadienyl ancillary ligands or are clusters with sulfur bridges.<sup>9</sup> There appears to be little evidence supporting strong sulfur-metal  $\pi$  bonding for the complexes that have been reported thus far.<sup>10</sup> Eliminating the propensity for  $\pi$  bonding with the metal should also lessen the tendency to form a  $C_s$  structure.<sup>7</sup> Herein we describe the synthesis of a novel bis(thiolate)-pyridine ligand and investigations of its binding preferences with group 4 and 5 transition metals. Although our expectations that, in comparison with their (ONO)MX<sub>2</sub> (M = Ti, Zr) and (ONO)TaX<sub>3</sub> analogues, the (SNS)MX<sub>2</sub> and (SNS)TaX<sub>3</sub> complexes do indeed strongly favor twisted,  $C_2$  geometries, the Ti and Zr amide complexes have not proven to be effective catalyst precursors for propylene polymerization. Thus, it was not possible to investigate stereocontrol in producing isotactic polypropylenes. The dynamic behavior, involving both

restricted rotation about the amide Ta–N bonds and interconversion between antipodes by inversion at Ta, has, however, been examined by NMR methods.

## RESULTS AND DISCUSSION

**Synthesis of the (SNS)H<sub>2</sub> Ligand and its Titanium and Zirconium Complexes.** Palladium-catalyzed cross couplings, used previously to prepare related LX<sub>2</sub> pincer ligands, are not generally suited to the direct synthesis of bis(thiophenol)-pyridine, due to poisoning of the Pd by sulfur. Moreover, common allyl or benzyl thioether protecting groups are easily cleaved by palladium, again leading to catalyst poisoning. A preliminary attempt to protect the thiophenol with an alkylmercaptopyropionate group, which had been reported to tolerate Suzuki coupling conditions, failed.<sup>11</sup> Fortunately, a methyl-protected phenyl sulfide proved stable to palladium-catalyzed Suzuki coupling conditions.

The desired ligand was synthesized in two steps from 2-(methylthio)phenylboronic acid and 2,6-dibromopyridine (Scheme 1). These reagents were subjected to Suzuki coupling conditions, which generated the protected (SNS)Me<sub>2</sub> (**1**) in 89% yield. Treatment of **1** with sodium 2-methyl-2-propane-

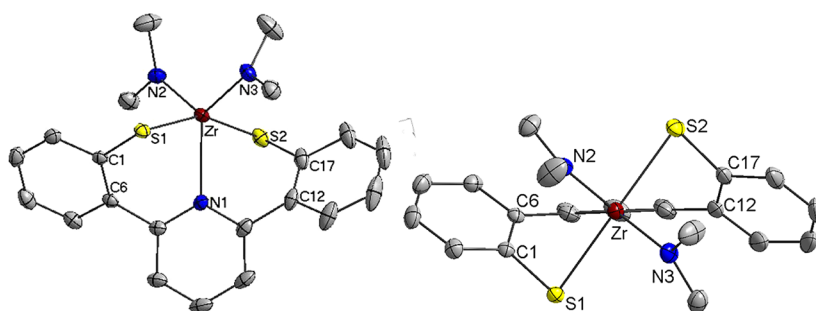


**Figure 1.** Front (left) and top (down the Zr–N1 bond, right) views of the structure of **4** with thermal ellipsoids at the 50% probability level. Hydrogen atoms are omitted for clarity. Selected bond lengths (Å) and angles (deg): Zr–S1, 2.5723(3); Zr–S2, 2.5528(3); Zr–N1, 2.3499(7) Zr–N2, 1.9995(8); Zr–N3, 2.0041(8); S1–C1, 1.7743(9); S2–C17, 1.7743(11); Zr–S1–C1, 88.40(3); Zr–S2–C17, 86.12(3); S1–Zr–S2, 156.934(9); N2–Zr–N3, 113.06(3); C1–C6–C12–C17, 71.993(81).

thiolate ( $\text{Me}_3\text{CSNa}$ ) at 160 °C for 4 h removed the protecting methyl group.<sup>12</sup> Acid workup afforded the moderately air-sensitive ligand  $(\text{SNS})\text{H}_2$  (**2**) in 68% yield. A distinctive broad peak observed in the  $^1\text{H}$  NMR spectrum at  $\delta$  4.66 corresponds to the thiol protons.

Titanium and zirconium dimethylamido complexes were prepared by salt metathesis and aminolysis, respectively (Scheme 2). Although  $^1\text{H}$  and  $^{13}\text{C}$  NMR spectroscopy support clean formation of  $(\text{SNS})\text{Ti}(\text{NMe}_2)_2$  (**3**), **3** decomposes in solution over 12 h to an insoluble red-brown solid as an intractable mixture of products. The zirconium complex  $(\text{SNS})\text{Zr}(\text{NMe}_2)_2$  (**4**) proved more stable, and X-ray-quality crystals were obtained by slow evaporation of pentane into a concentrated benzene solution of **4** at room temperature (Figure 1).

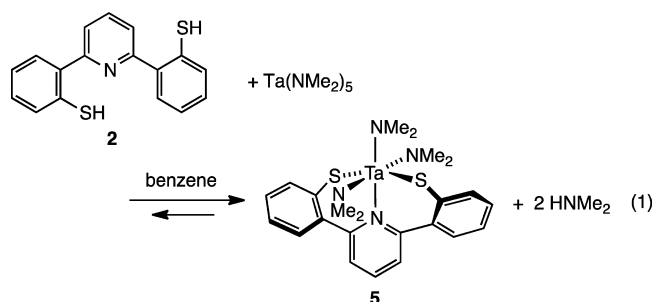
The relatively long Zr–S bond lengths of 2.67 and 2.56 Å confirm that sulfur is binding as an X-type ligand in **4** with little S lone pair-to-Zr  $\pi$  donation.<sup>8,10</sup> Previous work with six-coordinate  $(\text{ONO})\text{TaX}_3$  complexes demonstrated a preference for  $C_2$  binding modes when the ancillary X type ligands  $\pi$  donate, outcompeting the phenolate for  $\pi$  donation to tantalum.<sup>7a</sup> On the other hand, five-coordinate  $(\text{ONO})\text{TiX}_2$  complexes demonstrated a preference for  $C_s$  binding modes when the ancillary X type ligands  $\pi$  donate to titanium better than phenolate, despite the increased ring strain caused by this ligand geometry. Accordingly,  $(\text{ONO})\text{Ti}(\text{CH}_2\text{Ph})_2$  has  $C_2$  symmetry, while  $(\text{ONO})\text{Ti}(\text{NMe}_2)_2$  has  $C_s$  symmetry.<sup>4,7b</sup> Thus, a  $C_s$  geometry would be expected for five-coordinate **4**, rather than the observed  $C_2$  geometry, because the dimethylamido ancillary ligands of **4** are strong  $\pi$  donors. Instead, the long Zr–S and S–C bonds that force the six-membered chelate to adopt a severely nonplanar ring and (likely) steric preferences for the two dimethylamido groups to be roughly trans appear to override any electronic preferences arising from nitrogen  $\pi$  donation to zirconium, resulting in distinctly  $C_2$  twisting of the SNS ligand for **4**. Indeed, the 72.65° dihedral angle (C1–C6–C12–C17) between the two thiophenolate planes is larger than the corresponding dihedral angle for any  $C_2$ -symmetric ONO complex synthesized to date (52.70–69.24°).<sup>4,5,7</sup> The dihedral angle for **4** is smaller, however, than those for related  $C_2$ -symmetric bis(anilide)-pyridine and bis(phosphide)pyridine complexes (79.20–94.13°). These NNN and PNP ligands have aryl groups on the secondary pnictogens that further increase the steric bulk of the ligand and force an even greater dihedral twist.<sup>13</sup>

Attempts to prepare group 4 metal complexes with ancillary ligands other than dimethylamide have been unsuccessful to

date. Toluene elimination from tetrabenzyltitanium, -zirconium, and -hafnium in order to generate dibenzyl complexes resulted in the immediate precipitation of insoluble brown solids. Efforts to generate halogen-ligated complexes by treating  $(\text{SNS})\text{K}_2$  with group 4 metal chlorides or  $(\text{SNS})\text{H}_2$  with mixed chloro-amido compounds were also unsuccessful, as were reactions of **3** and **4** with 1 equiv or more of trimethylsilyl chloride. We hypothesize that the combination of weak sulfur-to-metal  $\pi$  donation and less bulky, weaker  $\pi$  donor ancillary ligands encourage oligomerization of these alkyl and chloro complexes through sulfur and/or chlorine bridges, ultimately leading to oligomerization to insoluble materials.

Neither **3** nor **4** was a competent precatalyst for propylene polymerization, likely due to decomposition during the activation process. Activation by methylaluminoxane (MAO) is expected to generate methyl cations  $[(\text{SNS})\text{MCH}_3]^+$  that would likely be even more unstable than the neutral dibenzyl complexes (vide supra).<sup>14</sup> Adding bulk to the ortho position of the ligand might stabilize the electron-deficient complex, while simultaneously inhibiting bridging through the sulfur lone pair.

**Preparation of Tantalum Complexes Supported by the Bis(thiophenolate)pyridine Ligand.** The tantalum complex  $(\text{SNS})\text{Ta}(\text{NMe}_2)_3$  (**5**) was prepared by aminolysis of  $\text{Ta}(\text{NMe}_2)_5$  with  $(\text{SNS})\text{H}_2$  (eq 1). Only a small amount of **5** is formed initially, but the reaction can be driven to completion by removing the volatile dimethylamine.



X-ray-quality crystals were obtained by diffusing pentane into a concentrated benzene solution of **5** at room temperature (Figure 2). The SNS fragment binds meridionally with  $C_2$  symmetry (as expected by analogy to the  $(\text{ONO})\text{Ta}(\text{NMe}_2)_3$  complex<sup>7a</sup> as well as **4** above), displaying an average Ta–S bond length of 2.49 Å and a dihedral angle of 79.9° (C1–C6–C12–C17). Both metrics are larger than the corresponding ones observed in  $(\text{ONO})\text{Ta}(\text{NMe}_2)_3$  (Ta–O bond length, 1.98 Å; dihedral angle, 59.7°) with longer S–Ta and C–S bond

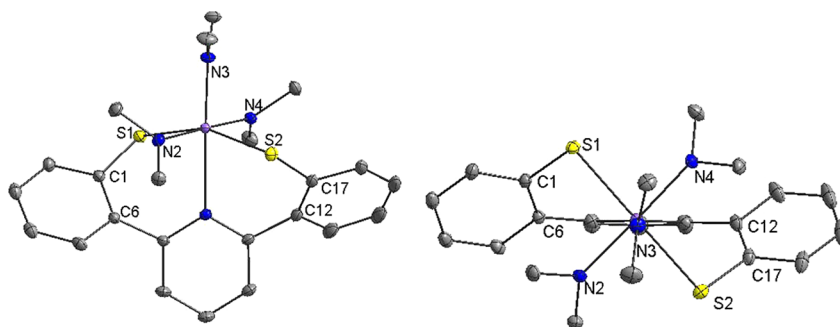


**Figure 2.** Front (left) and top (down the Zr–N1 bond, right) views of the structure of **5** with thermal ellipsoids at the 50% probability level. Hydrogen atoms are omitted for clarity. Selected bond lengths (Å) and angles (deg): Ta–S1, 2.4887(3); Ta–S2, 2.4823(3); Ta–N1, 2.3927(11); Ta–N2, 2.0264(11); Ta–N3, 1.9868 (11); Ta–N4, 2.0352(11); S1–C1, 1.7537(12); S2–C17, 1.7555(15); Ta–S1–C1, 101.79(4); Ta–S2–C17, 100.13(5); S1–Ta–S2, 158.011(11); N2–Ta–N4, 177.16(5); C1–C6–C12–C17, 79.853(112).

lengths forcing the six-membered chelate rings significantly nonplanar.

The dimethylamide groups of  $(\text{ONO})\text{Ta}(\text{NMe}_2)_3$  exhibit two sharp peaks by  $^1\text{H}$  NMR with a 12:6 ratio as expected from the solid-state structure at room temperature.<sup>7</sup> In contrast, **5** shows three distinct amide methyl peaks in the  $^1\text{H}$  NMR spectrum at  $\delta$  2.83 ( $\text{CH}_3^\alpha$ ), 3.22 ( $\text{CH}_3^\beta$ ), and 3.65 ( $\text{CH}_3^{\text{ax}}$ ) that integrate in a 6:6:6 ratio (Figure 3). Restricted rotation about

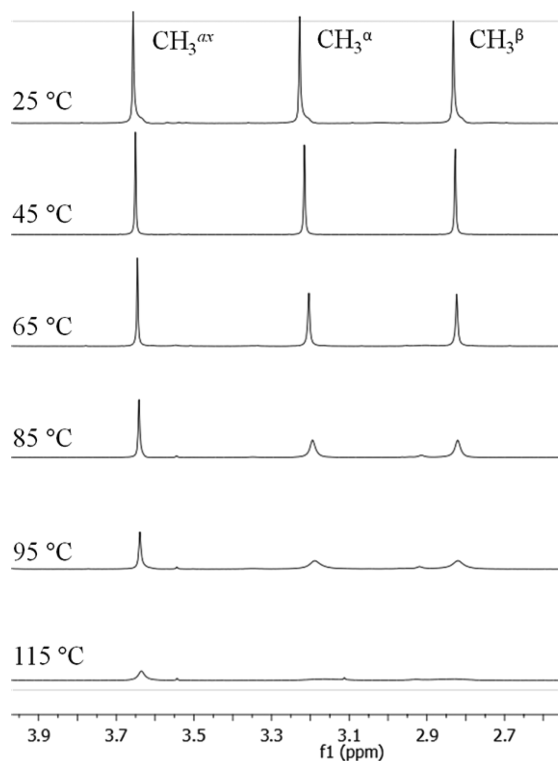
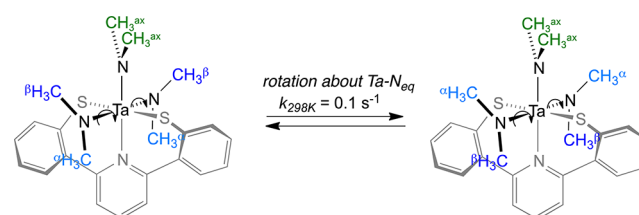


**Figure 3.** Variable-temperature  $^1\text{H}$  NMR of the alkyl region of **5**, showing peak exchange among A, B, and C.

the equatorial Ta–N(amide) bonds leads to an inequivalence between the “top” and “bottom” methyl groups of the equatorial amides (Scheme 3). A series of through-space and through-bond  $^1\text{H}$ ,  $^{13}\text{C}$ , and  $^{15}\text{N}$  2D NMR experiments confirmed the assignment of  $\text{CH}_3^\beta$  as top and  $\text{CH}_3^\alpha$  as bottom (see the Supporting Information).

Furthermore, 1D-NOE  $^1\text{H}$  NMR spectroscopy revealed a process exchanging the methyl groups in sites  $\alpha$  and  $\beta$ , likely

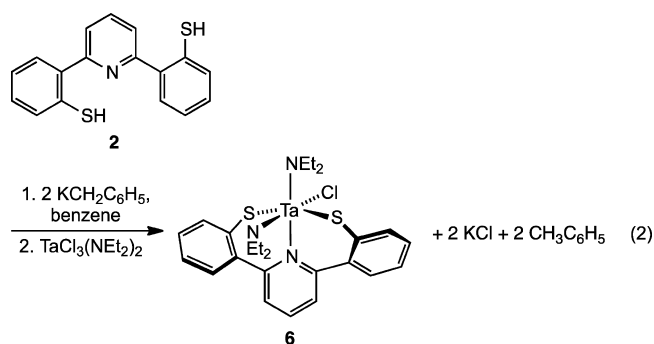
### Scheme 3



involving simple rotation of the equatorial Ta–N bond, as selectively exciting the protons of  $\text{CH}_3^\beta$  (2.83 ppm) resulted in magnetization resonance transfer to  $\text{CH}_3^\alpha$  (3.22 ppm) and vice versa. Cooling the sample to  $-10^\circ\text{C}$  slows this rotation, allowing estimation of the NOE contribution between  $\text{CH}_3^\alpha$  and  $\text{CH}_3^\beta$ . These data combined with a series of presaturation delay 1D-NOE experiments provided an exchange rate for equatorial amide methyls of  $0.11(2)\text{ s}^{-1}$  at 298 K.

Heating an NMR sample of **5** from 25 to  $115^\circ\text{C}$  leads to broadening of peaks attributable to  $\text{CH}_3^\alpha$  and that for  $\text{CH}_3^\beta$  (Figure 3). At the highest temperature these two peaks have coalesced and a notable broadening of the peak for  $\text{CH}_3^{\text{ax}}$  occurs, possibly an indication that relatively slow positional exchange between axial and equatorial amides is taking place. Exchange of  $\text{CH}_3^\alpha$ ,  $\text{CH}_3^\beta$ , and  $\text{CH}_3^{\text{ax}}$  might be achieved through conversion of the meridionally bound ligand to a facial binding mode followed by rotation about the  $\text{C}_3$  (N1–N2–N3) axis (see the Supporting Information). This meridional to facial rearrangement would require substantial strain on the SNS fragment but is not without precedence: a similar explanation was proposed in the exchange of axial and equatorial groups at room temperature for  $(\text{ONO})\text{TaMe}_3$ . Additionally, the solid-state structure of the dimer  $[(\text{ONO})\text{Ta}(\text{OH})_2(\mu_2\text{-O})_2]$  has facially bound ONO fragments.<sup>7,16</sup> Alternatively, dissociation of the pyridine of SNS and rearrangement via a five-coordinate species might be occurring.<sup>15</sup>

To further assess the conformational flexibility of the SNS framework, a new complex,  $(\text{SNS})\text{TaCl}(\text{NET}_2)_2$  (**6**), was synthesized by salt metathesis of  $(\text{SNS})\text{K}_2$  with  $\text{TaCl}_3(\text{NET}_2)_2$  (eq 2). Our interest in this compound stems from the fact that the diastereotopic methylene protons of the diethylamide coligands of **6** exchange only if the molecule can undergo interconversion between  $\text{C}_2$  antipodes. Crystallization by diffusion of pentane into benzene gave crystals suitable for X-ray structural analysis (Figure 4). The metrics of **6** are nearly identical to those of **5**, despite having a chloride in place of an amide and a more acute C1–C6–C12–C17 dihedral angle of



71.42° (vs 79.9° in **5**). Here again the strained six-membered chelate rings dominate the geometric preference for  $C_2$  coordination in **6**, in contrast with the ONO ligand system, which assumes  $C_s$  symmetry in  $(\text{ONO})\text{TaCl}(\text{NMe}_2)_2$  to maximize phenolate  $\pi$  bonding to Ta.<sup>7</sup>

The room-temperature  $^1\text{H}$  NMR spectrum of **6** is composed of several nondescript broad peaks (Figure 5). On cooling to  $-50^\circ\text{C}$  a more informative  $^1\text{H}$  NMR spectrum emerges, revealing separate signals for some of the geminal protons of the methylene groups of the diethylamide ligands, appearing as multiplets (due to apparently comparable geminal and methyl coupling) for the methylene protons with relative intensities of 2:1:[1:2(overlapping)]:1:1. Assignments as shown in Scheme 4 were further established by 2D NMR experiments (see the Supporting Information). The four-multiplet pattern of methylene protons  $\text{H}^{\text{B}1}$ ,  $\text{H}^{\text{B}2}$ ,  $\text{H}^{\text{B}3}$ , and  $\text{H}^{\text{B}4}$  further indicates both slow rotation of the equatorial Ta–N(amide) bond (as observed for **5**), and slow inversion at Ta. On the other hand, the equivalencing of  $\text{H}^{\text{A}1}/\text{H}^{\text{A}1'}$  and  $\text{H}^{\text{A}2}/\text{H}^{\text{A}2'}$  leading to only two broad peaks of relative intensity 2 implies that relatively rapid axial Ta–N(amide) bond rotation occurs at  $-50^\circ\text{C}$ . At  $-75^\circ\text{C}$  these two broad peaks split further, and although we were not able to obtain satisfactory spectra at lower temperatures, we anticipate that these signals would continue to sharpen into four multiplets of intensities 1:1:1:1 (analogous to those for the equatorial amide methylenes) as rotation of the axial amide Ta–N bond becomes slow on the NMR time scale. Further upfield at the lower temperatures are separate triplets for the two methyl groups  $\text{CH}_3^\alpha$  and  $\text{CH}_3^\beta$  of the equatorial diethylamide ligand and two overlapping triplets for the less

well resolved  $\text{CH}_3^\alpha$  methyl groups of the axial diethylamide. At  $100^\circ\text{C}$  a simple  $^1\text{H}$  NMR spectrum emerges that consists of two quartets (equatorial and axial amide methylenes) and two triplets (equatorial and axial amide methyls) with relative intensities of 4:4:6:6.

The  $^1\text{H}$ – $^1\text{H}$  ROESY of **6** at  $-50^\circ\text{C}$  reveals exchange *does* occur between  $\text{H}^{\text{B}1}$  and  $\text{H}^{\text{B}3}$  and between  $\text{H}^{\text{B}2}$  and  $\text{H}^{\text{B}4}$  indicative of relative fast equatorial amide Ta–N rotation but, importantly, no significant exchange between  $\text{H}_{\text{B}1}$  and  $\text{H}_{\text{B}2}$  or between  $\text{H}^{\text{B}3}$  and  $\text{H}^{\text{B}4}$ , indicating that inversion at Ta is not occurring on the ROESY time scale at this temperature. Thus, at least at  $-50^\circ\text{C}$ , equatorial amide rotation is faster than inversion at Ta. At intermediate temperatures the spectra are not readily interpreted, however. From the spectrum at  $25^\circ\text{C}$  we can estimate from the coalescence of the two methyl groups  $\text{CH}_3^\alpha$  and  $\text{CH}_3^\beta$  of the equatorial diethylamide ligand that the Ta–N rotational barrier is approximately 13.4(1) kcal/mol at 298 K, corresponding to a rate of  $900\text{ s}^{-1}$ .<sup>17</sup> An approximate fit for exchange of  $\text{H}^{\text{A}1}$  with  $\text{H}^{\text{A}1'}$  yields an axial diethylamide ligand Ta–N rotational barrier of 9.4(1) kcal/mol (at 200 K), corresponding to a rate of  $560\text{ s}^{-1}$ . At the highest temperature both amide rotation and inversion at Ta must be relatively fast in order to make both ethyl groups of each of the diethyl amide ligands equivalent: i.e., both  $\text{H}^{\text{B}1}$  exchange with  $\text{H}^{\text{B}3}$  (rotation) and  $\text{H}^{\text{B}1}$  exchange with  $\text{H}^{\text{B}2}$  (inversion at Ta) must be fast. The same holds true for  $\text{H}^{\text{B}2}$  exchange with  $\text{H}^{\text{B}4}$  (rotation) and  $\text{H}^{\text{B}3}$  exchange with  $\text{H}^{\text{B}4}$  (inversion at Ta). Unfortunately, the data are not precise enough to allow deconvolution of the separate contributions of the amide rotation and inversion at Ta to the line shape of signals for these four methylene protons at intermediate temperatures. Thus, we conservatively estimate that the barrier to inversion is comparable to that for rotation, at least at the higher temperatures: i.e.,  $\Delta G_{\text{inv}}^\ddagger \approx 14(1)\text{ kcal/mol}^{-1}$ . Thus, these NMR data indicate that although the longer Ta–S and S–C bonds result in considerable ring strain in SNS complexes, the framework is nonetheless flexible enough to allow inversion at Ta to interconvert antipodes with a moderate barrier for **6**.

## CONCLUSIONS

A novel bis(thiophenol)pyridine ligand has been synthesized and metalated with Ti(IV), Zr(IV), and Ta(V) precursors to form dialkylamido and trialkylamido complexes. Solid-state

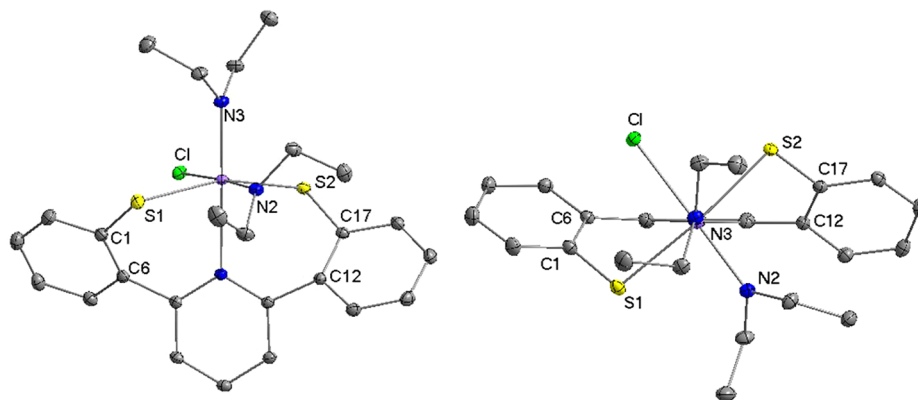


**Figure 4.** Structure of **6** with thermal ellipsoids at the 50% probability level. The left image is a front view, and the right image is a top view down the N3–Ta–N1 bond. Hydrogen atoms are omitted for clarity. Selected bond lengths (Å) and angles (deg): Ta–S1, 2.42715(19); Ta–S2, 2.47717(19); Ta–N1, 2.3911(2); Ta–N2, 1.9873(6); Ta–N3, 1.9538(6); Ta–Cl, 2.45843(19); S1–C1, 1.7615(8); S2–C17, 1.7550(7); Ta–S1–C1, 103.88(2); Ta–S2–C17, 102.814(2); S1–Ta–S2, 160.364(6); N2–Ta–Cl, 176.970(18); C1–C6–C12–C17, 71.415(59).

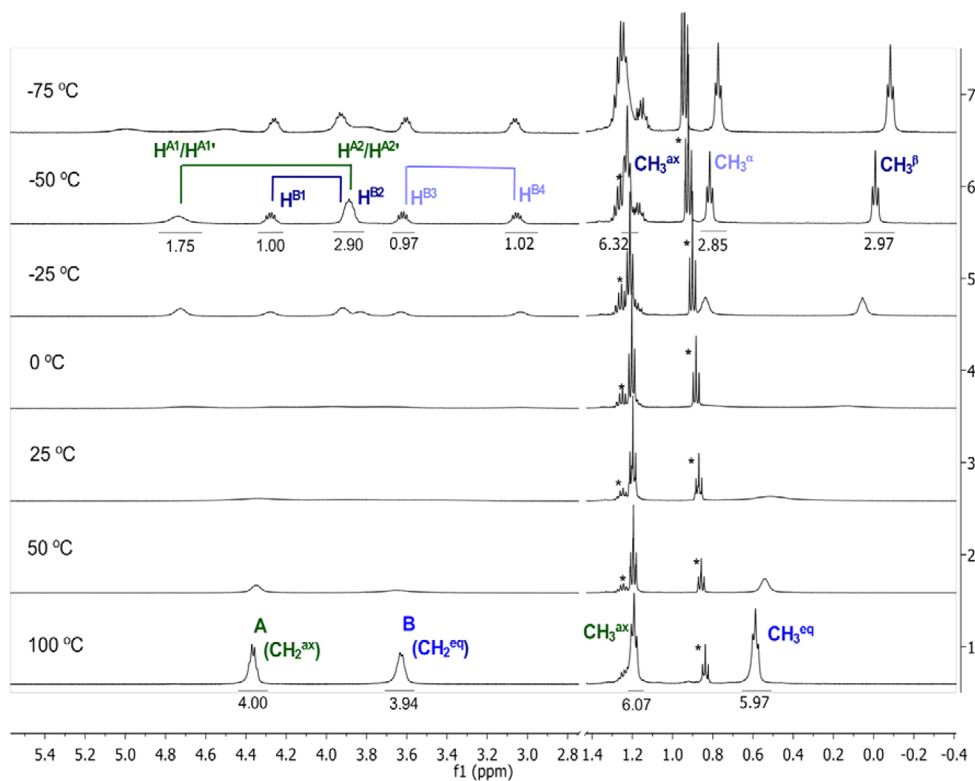


**Figure 5.**  $^1\text{H}$  NMR of **6** from  $-50$  to  $100$   $^\circ\text{C}$  in  $d_8$ -toluene. Integrals are shown beneath the spectra. The labeling corresponds to that in Scheme 4. Spectra are not shown on the same vertical scale due to the low solubility of **6** at colder temperatures. Asterisks denote an impurity observed at 0.84 and 1.24 ppm (attributable to residual  $\text{Ta}(\text{NEt}_2)_2\text{Cl}_3$ ) that retains solubility at lower temperatures, leading to perceived signal amplification.

structures of Zr(IV) complex **4** and Ta(V) complexes **5** and **6** show a meridional coordination having a twisted  $C_2$  symmetric arrangement of the SNS ligand with the largest dihedral angles for a bis(chalcogenate)pyridine ligand system thus far. Increased ring strain of the six-membered thiophenolate rings resulting from long Ta–S and C–S bond lengths and acute bond angles at sulfur is a major factor influencing this coordination mode, overriding any alternative coordination that maximizes  $\pi$  bonding between the metal and chalcogenide, as is seen for the ONO analogues. The  $C_2$  symmetry of **5** persists in solution at room temperature with relatively rapid rotation about the amide Ta–N bonds, while at higher temperatures all three amide ligands exchange, implying that the SNS framework likely exhibits sufficient flexibility to allow access to trigonal-prismatic intermediates with a facial coordination of the  $\text{LX}_2$  chelate. Variable-temperature studies for **6**, which possesses diastereomeric protons for the methylene groups of the two diethylamide ligands, confirm that the complex interconverts between antipodes with a moderate barrier for inversion at Ta. Although titanium and zirconium complexes proved to be poor catalyst precursors for propylene polymerization, their structures and the fluxional behavior of the tantalum complexes have provided additional insights into the coordination preferences for this class of  $\text{LX}_2$  pincer ligands.

## EXPERIMENTAL SECTION

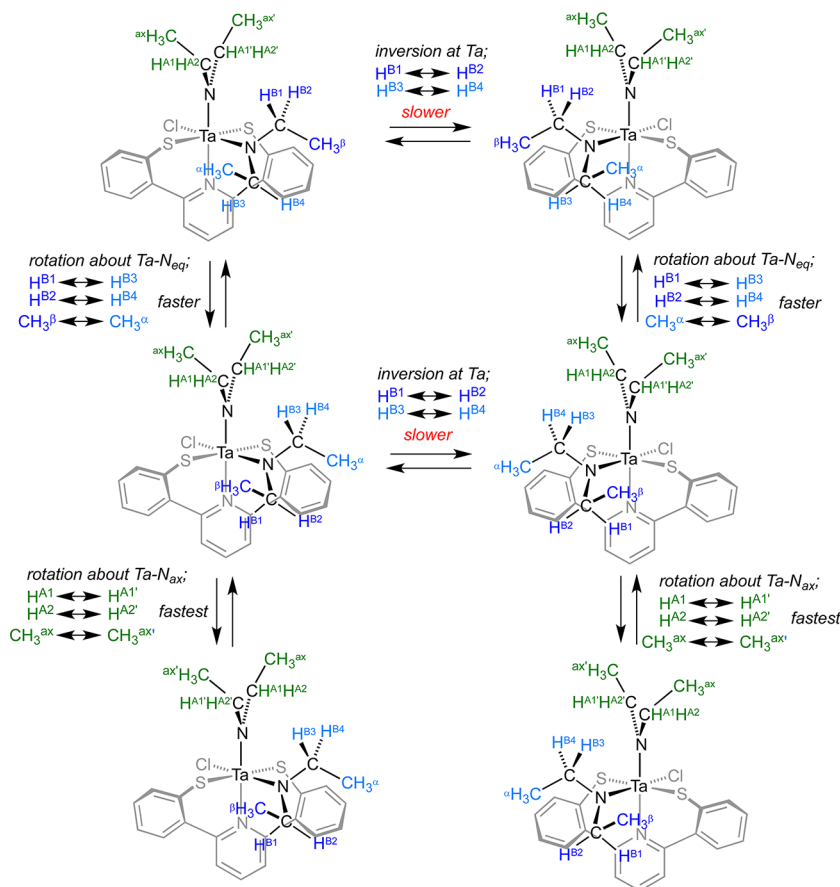
**General Considerations.** All air- and moisture-sensitive compounds were manipulated using standard high-vacuum-line, Schlenk, or cannula techniques or in a glovebox under a nitrogen atmosphere. Benzylpotassium (KBn) was prepared according to literature methods.<sup>18</sup>  $\text{Zr}(\text{NMe}_2)_4$  and  $\text{Ta}(\text{NMe}_2)_5$  were purchased from Strem

Chemicals and sublimed prior to use.  $\text{TiCl}_2(\text{NMe}_2)_2$  and  $\text{TaCl}_3(\text{NEt}_2)_2$  were prepared according to literature methods.<sup>19,20</sup> DMF was dried by the Grubbs method<sup>21</sup> and stored over 3 Å molecular sieves for 36 h prior to use. All other solvents for air- and moisture-sensitive reactions were dried over sodium benzophenone ketyl and stored over titanocene where compatible or dried by the method of Grubbs et al.<sup>21</sup> Benzene- $d_6$  and toluene- $d_8$  were purchased from Cambridge Isotopes and dried over sodium benzophenone ketyl. Methylene chloride- $d_2$  was purchased from Cambridge Isotopes, distilled from calcium hydride, and filtered through a plug of activated alumina. All other materials were used as received.  $^1\text{H}$  and  $^{13}\text{C}$  NMR spectra were recorded on Varian Mercury 300, Varian Inova 500, or Varian Inova 600 spectrometers at room temperature unless otherwise indicated. Chemical shifts are reported with respect to internal solvent: 7.16 and 128.38 (t) ppm ( $\text{C}_6\text{D}_6$ ), 2.08 and 25 ppm ( $d_8$ -tol), and 5.32 and 54 (q) ppm ( $\text{CD}_2\text{Cl}_2$ ) for  $^1\text{H}$  and  $^{13}\text{C}$  data, respectively.

**Synthesis of (SNS)Me<sub>2</sub> (1).** *trans*-Dichlorobis-(triphenylphosphine)palladium(II) (1.22 g, 0.0018 mol) was placed in a 500 mL thick-walled glass flask fitted with a Teflon valve and dissolved in 200 mL of 1,2-dimethoxyethane. To this mixture was added 2-(methylthio)phenylboronic acid (8.820 g, 0.053 mol) and 2,6-dibromopyridine (4.14 g, 0.018 mol). Potassium carbonate (7.41 g 0.70 mol) was dissolved in 50 mL of water and added to the solution. The Schlenk tube was sealed and heated to 85  $^\circ\text{C}$  for 12 h. Purification by column chromatography (98/2 hexanes/ethyl acetate) afforded **1** as an off-white solid (5.06 g, 15.6 mmol, 86.7% yield).  $^1\text{H}$  NMR (300 MHz,  $\text{CD}_2\text{Cl}_2$ ):  $\delta$  7.84 (dd,  $J = 8.2, 7.4$  Hz, 1H), 7.60 (dd,  $J = 4.4, 3.3$  Hz, 4H), 7.46–7.37 (m, 4H), 7.34–7.23 (m, 2H) (aryl); 2.43 (s, 6H) ( $\text{S}(\text{CH}_3)$ ).  $^{13}\text{C}$  NMR (75 MHz,  $\text{CD}_2\text{Cl}_2$ ):  $\delta$  158.01, 140.06, 137.93, 136.40, 130.53, 129.18, 126.46, 124.14, 122.89 (aryl); 16.80 ( $\text{CH}_3$ ).

**Synthesis of (SNS)H<sub>2</sub> (2).** In a dry 50 mL thick-walled glass flask fitted with a Teflon valve were placed **1** (76 mg, 0.235 mmol) and 2-methyl-2-propanethiol (211 mg, 1.87 mmol) under argon. The tube was then evacuated overnight and refilled with argon. Dry DMF (10 mL) was added via cannula. The vessel was sealed, and the reaction mixture was stirred for 4 h at 160  $^\circ\text{C}$ . The reaction mixture was cooled

Scheme 4



to 0 °C for 30 min. Under an argon purge, hydrochloric acid (5 mL, 3M) was added at 0 °C. The solution was transferred to a 200 mL beaker containing hydrochloric acid (10 mL, 3 M) and  $\text{CH}_2\text{Cl}_2$  (100 mL). The aqueous layer was washed twice with  $\text{CH}_2\text{Cl}_2$  (100 mL). Organic layers were combined, and the solvent was removed under reduced pressure. The solid product was taken into an inert-atmosphere glovebox, where it was filtered through a small plug of silica with hexanes. Hexanes were removed from the filtrate to afford **2** as an off-white solid (47 mg, 0.16 mmol 67%).  $^1\text{H}$  NMR (300 MHz,  $\text{CD}_2\text{Cl}_2$ ):  $\delta$  7.93 (t, 1H), 7.70–7.50 (m, 4H), 7.47–7.34 (m, 2H), 7.33–7.19 (m, 4H) (aryl), 4.66 (bs, 2H) (SH).  $^{13}\text{C}$  NMR (75 MHz,  $\text{CD}_2\text{Cl}_2$ ):  $\delta$  157.97, 138.44, 138.17, 132.28, 131.50, 131.01, 129.43, 126.13, 122.72 (aryl). Anal. Calcd for  $\text{C}_{17}\text{H}_{13}\text{NS}_2$ : C, 69.12; H, 4.44; N, 4.74. Found: C, 67.89; H, 4.39; N, 4.63. This compound appears to be sensitive to air oxidation at sulfur. Calcd for  $\text{C}_{17}\text{H}_{13}\text{NS}_2\text{O}_{0.2}$  (estimated on the basis of partial oxidation at sulfur): C, 67.89; H, 4.36; N, 4.66. HRMS (FAB+):  $\text{C}_{17}\text{H}_{13}\text{NS}_2$  [M + H] calcd mass 296.0568, measd mass 296.0546.

**Synthesis of (SNS)Ti(NMe<sub>2</sub>)<sub>2</sub> (3).** In an inert-atmosphere glovebox, **2** (9.0 mg, 0.030 mmol) was dissolved in benzene (2 mL) and benzylpotassium (7.9 mg, 0.061 mmol) was added. The solution was stirred for 1 h at room temperature, after which  $\text{TiCl}_2(\text{NMe}_2)_2$  (6.2 mg, 0.030 mmol) was added and the mixture allowed to react for 2 h. The solution was filtered, and solvent was removed under vacuum, leaving a red-brown powder. The solid was redissolved in  $\text{C}_6\text{D}_6$ , showing the clean formation of **3** (5.5 mg, 0.013 mmol, 42.6%).  $^1\text{H}$  NMR (500 MHz,  $\text{C}_6\text{D}_6$ ):  $\delta$  7.63 (dd,  $J = 7.8, 0.8$  Hz, 2H), 7.10 (dd,  $J = 7.7, 1.3$  Hz, 2H), 7.01 (t, 1H), 6.88 (td,  $J = 7.6, 1.5$  Hz, 2H), 6.80 (d,  $J = 7.8$  Hz, 2H), 6.79 (td,  $J = 7.6, 1.3$  Hz, 2H) (aryl); 2.98 (s, 6H) ( $\text{N}(\text{CH}_3)_2$ ).  $^{13}\text{C}$  NMR (126 MHz,  $\text{C}_6\text{D}_6$ ):  $\delta$  156.18, 143.27, 139.96, 138.39, 134.33, 129.88, 129.61, 124.37, 123.62 (aryl); 45.33 ( $\text{N}(\text{CH}_3)_2$ ).

**Synthesis of (SNS)Zr(NMe<sub>2</sub>)<sub>2</sub> (4).** In an inert-atmosphere glovebox, **2** (5.1 mg, 0.017 mmol) was dissolved in benzene (5 mL) and the solution was transferred to a vial containing  $\text{Zr}(\text{NMe}_2)_4$  (4.8 mg, 0.017 mmol). The solution immediately turned bright yellow with some precipitate forming. The reaction mixture was stirred for 1 h, after which solvent and formed dimethylamine were removed under vacuum. Benzene was added to the solution, and the precipitate was filtered off to produce pure **4** (5.0 mg, 0.011 mmol, 62%). X-ray-quality crystals were grown by slow diffusion of pentane into a benzene solution of **4**.  $^1\text{H}$  NMR (300 MHz,  $\text{C}_6\text{D}_6$ ):  $\delta$  7.83 (dd,  $J = 7.7, 1.2$  Hz, 2H), 7.04–6.97 (m, 3H), 6.93 (ddd,  $J = 7.9, 7.3, 1.7$  Hz, 2H), 6.80 (td, 2H), 6.74 (d,  $J = 7.9$  Hz, 2H) (aryl); 2.68 (s, 12H) ( $\text{N}(\text{CH}_3)_2$ ).  $^{13}\text{C}$  NMR (126 MHz,  $\text{C}_6\text{D}_6$ ):  $\delta$  156.26, 140.78, 140.18, 137.63, 137.01, 130.33, 129.74, 123.84, 123.71 (aryl); 40.05 ( $\text{N}(\text{CH}_3)_2$ ). Anal. Calcd for  $\text{C}_{21}\text{H}_{23}\text{N}_3\text{S}_2\text{Zr}$ : C, 53.35; H, 4.90; N, 8.89. Found: C, 53.48; H, 4.97; N, 8.46.

**Synthesis of (SNS)Ta(NMe<sub>2</sub>)<sub>3</sub> (5).** In an inert-atmosphere glovebox, **2** (15.0 mg, 0.051 mmol) was dissolved in  $\text{C}_6\text{D}_6$  (1 mL) and the solution was transferred to a vial containing  $\text{Ta}(\text{NMe}_2)_5$  (20.4 mg, 0.051 mmol). The solution immediately turned bright orange, and  $^1\text{H}$  NMR confirmed 50% product formation. Solvent and formed dimethylamine were removed under vacuum, and the orange solid was redissolved in  $\text{C}_6\text{D}_6$  and allowed to react an additional 1 h, affording **5** (28.2 mg, 0.046 mmol, 91%). X-ray-quality crystals were grown by slow diffusion of pentane into a concentrated benzene solution of **5**.  $^1\text{H}$  NMR (300 MHz,  $\text{C}_6\text{D}_6$ ):  $\delta$  7.87–7.68 (m, 2H), 7.13–7.07 (m, 2H), 7.04–6.93 (m, 3H), 6.88–6.79 (m, 4H), 3.69 (s, 6H), 3.30 (s, 6H), 2.89 (s, 6H).  $^{13}\text{C}$  NMR (126 MHz,  $\text{C}_6\text{D}_6$ ):  $\delta$  157.96, 145.14, 142.44, 137.46, 132.81, 129.75, 127.23, 125.58, 122.79 (aryl); 50.14, 47.79, 44.43 ( $\text{N}(\text{CH}_3)_2$ ). Anal. Calcd for  $\text{C}_{23}\text{H}_{29}\text{N}_4\text{S}_2\text{Ta}$ : C, 45.54; H, 4.82; N, 9.24. Found: C, 46.27; H, 4.82; N, 8.19. This compound is very air- and moisture-sensitive. Despite repeated attempts, satisfactory combustion analysis could not be obtained.

**Synthesis of (SNS)TaCl(NEt<sub>2</sub>)<sub>2</sub> (6).** In an inert-atmosphere glovebox, **2** (5 mg, 0.017 mmol) was dissolved in C<sub>6</sub>D<sub>6</sub> (1 mL) and benzylpotassium (4.4 mg, 0.35 mmol) was added. The solution was stirred for 1 h, after which TaCl<sub>3</sub>(NEt<sub>2</sub>)<sub>3</sub> (7.3 mg, 0.017 mmol) was added to the solution and the mixture allowed to react for 2 h. <sup>1</sup>H NMR showed formation of **6** with some residual impurities from the Ta starting material (9.0 mg, 0.014, 81%). Solvent and diethylamine were removed under vacuum, leaving an orange powder. The solid was redissolved in benzene and crystallized by slow diffusion of pentane into the solution. <sup>1</sup>H NMR (500 MHz, d<sub>8</sub>-tol, -50 °C): δ 7.48–7.42 (m, 2H), 6.88–6.80 (m, 6H), 6.78–6.67 (m, 3H), 4.23 (dq (broad), J = 427.2 Hz, 4H), 4.12 (dq, J = 198.8, 6.9 Hz, 2H), 3.25 (dq, J = 283.7, 6.9 Hz, 2H), 1.14 (dd, J = 6.8 Hz, 6H), 0.73 (dd, J = 6.9 Hz, 3H), -0.09 (dd, J = 7.2 Hz, 3H). <sup>13</sup>C NMR (126 MHz, d<sub>8</sub>-tol, -50 °C): δ 158.90, 157.27, 145.32, 143.96, 142.61, 142.21, 138.68, 132.42, 131.03, 130.88, 128.70, 127.69, 125.13, 124.34 (aryl); 49.23, 48.65, 48.05 (CH<sub>2</sub>); 23.52, 14.01, 11.45 (CH<sub>3</sub>). Anal. Calcd for C<sub>25</sub>H<sub>31</sub>ClN<sub>3</sub>S<sub>2</sub>Ta: C, 45.91; H, 4.78; N, 6.42. Found: C, 48.98; H, 4.24; N, 3.55. As isolated, this compound is obtained as a mixture of approximately 80% **6** and 20% TaCl<sub>3</sub>(NEt<sub>2</sub>)<sub>3</sub> (NMR). Despite repeated attempts, satisfactory combustion analysis could not be obtained.

## ■ ASSOCIATED CONTENT

### Supporting Information

CIF files giving X-ray crystallographic data for compounds **4**–**6**, figures giving 1D-NOE and 2D NMR spectra for **5** and **6**, and text giving details of the synthesis of a second protected thiol compound and attempts to use it in carbon coupling reactions. This material is available free of charge via the Internet at <http://pubs.acs.org>.

## ■ AUTHOR INFORMATION

### Corresponding Author

\*E-mail: [bercaw@caltech.edu](mailto:bercaw@caltech.edu).

### Notes

The authors declare no competing financial interest.

## ■ ACKNOWLEDGMENTS

This work was supported by a KAUST Center-In-Development Grant to King Fahd University of Petroleum and Minerals (Dhahran, Saudi Arabia) and the USDOE Office of Basic Energy Sciences (Grant No. DE-FG03-85ER13431). We thank Ian A. Tonks and Matthew S. Winston for helpful discussions related to the research present in this paper. We also thank Lawrence M. Henling and Michael W. Day of Caltech for solving crystal structures. The Bruker KAPPA APEXII X-ray diffractometer was purchased via an NSF CRIF:MU award to the California Institute of Technology (CHE-0639094).

## ■ REFERENCES

- (1) (a) Facts and Figures. *Chem. Eng. News* **2007**, *85*, 55; (b) Coates, G. W. *Chem. Rev.* **2000**, *100*, 1223.
- (2) (a) Resconi, L.; Cavallo, L.; Fait, A.; Piemontesi, F. *Chem. Rev.* **2000**, *100* (4), 1253. (b) Fink, G.; Steinmetz, B.; Zechlin, J.; Przybyla, C.; Tesche, B. *Chem. Rev.* **2000**, *100*, 1377. (c) Kaminsky, W.; Arndt, M. *Adv. Polym. Sci.* **1997**, *127*, 143. (d) Andresen, A. C.; H. G.; Herwig, J.; Kaminsky, W.; Merck, A.; Mottweiler, R.; Rein, J.; Sinn, H. V.; H. J. *Angew. Chem., Int. Ed. Engl.* **1976**, *15*, 630.
- (3) (a) Chan, M. C. W.; Tam, K.-H.; Zhu, N.; Chiu, P.; Matsui, S. *Organometallics* **2006**, *25* (3), 785. (b) Chum, P. S.; Swogger, K. W. *Prog. Polym. Sci.* **2008**, *33*, 797. (c) Gibson, V. C.; Spitzmesser, S. K. *Chem. Rev.* **2003**, *103*, 283. (d) Britovsek, G. J. P.; Gibson, V. C.; Wass, D. F. *Angew. Chem., Int. Ed.* **1999**, *38*, 428.
- (4) Agapie, T.; Henling, L. M.; DiPasquale, A. G.; Rheingold, A. L.; Bercaw, J. E. *Organometallics* **2008**, *27*, 6245.
- (5) Golisz, S. R.; Bercaw, J. E. *Macromolecules* **2009**, *42*, 8751.

(6) Weinberg, D. R.; Hazari, N.; Labinger, J. A.; Bercaw, J. E. *Organometallics* **2010**, *29*, 89.

(7) (a) Tonks, I. A.; Henling, L. M.; Day, M. W.; Bercaw, J. E. *Inorg. Chem.* **2009**, *48*, 5096. (b) Tonks, I. A.; Bercaw, J. E. Unpublished results.

(8) Nakayama, Y.; Miyamoto, K.; Ueyama, N.; Nakamura, A. *Chem. Lett.* **1999**, *28*, 391.

(9) Stephan, D. W.; Nadasdi, T. T. *Coord. Chem. Rev.* **1996**, *147*, 147.

(10) Corwin, D. T.; Corning, J. F.; Koch, S. A.; Millar, M. *Inorg. Chim. Acta* **1995**, *229*, 335.

(11) (a) Zeysing, B.; Gosch, C.; Terfort, A. *Org. Lett.* **2000**, *2*, 1843.

(b) Hsung, R. P.; Babcock, J. R.; Chidsey, C. E. D.; Sita, L. R. *Tetrahedron Lett.* **1995**, *36*, 4525.

(12) Pinchart, A.; Dallaire, C. L.; Van Bierbeek, A.; Gingras, M. *Tetrahedron Lett.* **1999**, *40*, 5479.

(13) (a) Tonks, I. A.; Tofan, D.; Weintrob, E. C.; Agapie, T.; Bercaw, J. E. Submitted for publication. (b) Winston, M. S. B.; Bercaw, J. E. *Organometallics* **2010**, *29*, 6408.

(14) Zurek, E.; Ziegler, T. *Prog. Polym. Sci.* **2004**, *29*, 107.

(15) Berry, R. S. *J. Chem. Phys.* **1960**, *32*, 933.

(16) Agapie, T.; Day, M. W.; Bercaw, J. E. *Organometallics* **2008**, *27*, 6123.

(17) (a) Friebolin, H. *Dynamic NMR Spectroscopy Basic One- and Two-Dimensional NMR Spectroscopy*, 4th ed.; Wiley-VCH: Weinheim, Germany, 2005; p 311. (b) Values for ΔG<sup>‡</sup> were calculated at ±10 K, which is taken as the uncertainty.

(18) Bailey, P. J.; Coxall, R. A.; Dick, C. M.; Fabre, S.; Henderson, L. C.; Herber, C.; Liddle, S. T.; Lorono-Gonzalez, D.; Parkin, A.; Parsons, S. *Chem. Eur. J.* **2003**, *9*, 4820.

(19) Benzing, E.; Kurnicker, W. *Chem. Ber.* **1961**, *94*, 2263.

(20) Chao, Y. W.; Polson, S.; Wiglen, D. E. *Polyhedron* **1990**, *9*, 2709.

(21) Pangborn, A. B.; Giardello, M. A.; Grubbs, R. H.; Rosen, R. K.; Timmers, F. J. *Organometallics* **1996**, *15*, 1518.